An Observational and Numerical Study of Blocking Episodes near South America

ERNESTO H. BERBERY*

Department of Meteorology, University of Utah, Salt Lake City, Utah

MARIO N. NÚÑEZ

Departamento de Meteorología, Universidad de Buenos Aires, Consejo Nacional de Investigaciones Científicas y Técnicas

(Manuscript received 23 November 1988, in final form 8 June 1989)

ABSTRACT

European Centre for Medium-range Weather Forecasts analyses during June 1985 are used to characterize the flow in the South America sector during a typical blocking episode. Numerical experiments are performed using a hemispheric shallow-water model to test whether such blocking episodes can be a result of local resonance between forced Rossby waves generated by the Andes Mountains and by an upstream forcing.

It appears that while blocks generated in the Atlantic Ocean may respond to this mechanism from the beginning, the more frequent ones that develop from a ridge that advances from the Pacific Ocean may also benefit from it in the intensification and maintenance stages.

1. Introduction

Blocking occurs frequently in the region to the southeast of South America (van Loon 1956; Trenberth and Mo 1985). Blocking episodes have a large influence upon the weather in this region as they provide conditions favorable for cyclogenesis to the north of them (Grandoso and Núñez 1955), and due to the frequent presence of a cutoff low they can produce widespread rain and flooding (Taljaard 1972). On the other hand, Malaka and Núñez (1980), showed that the drought that ravaged the southern Argentine plains in 1962 was the consequence of repeated blocking in the South Atlantic. These two results are not inconsistent: drought or intense rainfall there depends upon the location of the affected region with respect to the block. Blocking episodes have also been related to the presence of cold spells (Taljaard 1972) and enhancement of the air pollution over Santiago de Chile (Rutllant and Fuenzalida 1987).

While blocks in the Northern Hemisphere have been studied extensively (e.g., Shukla and Mo 1983; Dole and Gordon 1983; Dole 1986) and those in the Australian–New Zealand region have been as well (e.g., Baines 1983; Trenberth 1986; Mo et al. 1987), few details are known about the origin and maintenance of blocks in the South American region. It has been observed that some ridges which advance from the Pacific Ocean across the South American continent may intensify, become stationary and then develop into a block. As several authors point out, even if the initial high weakens, another high may replace it in the same place. A second mechanism for blocking activity is the initiation and consolidation of the blocking high in the Atlantic Ocean (Grandoso and Núñez 1955).

Kalnay–Rivas and Merkine (1981, hereafter referred to as KRM) suggest that local resonance due to the interaction between forced Rossby waves generated by one source and forcing by a second source downstream of the first one may be responsible for blocking activity. Although in this paper we will consider only orographic forcing, the forcing could also be due to other sources such as land–sea contrast, sea surface temperature anomalies, or a region where frequent cyclogenesis occurs. According to this mechanism, for the Rossby waves to develop into a block downstream of the second forcing region, the first one must be such that it enhances the flow associated with the second one. In particular, if the second forcing is a mountain, the flow over it should be equatorward. The numerical experiments of KRM were performed with a barotropic model in a long channel with a Gaussian type mountain and cyclonic vorticity pulses generated upstream of the mountain. They suggest that this mechanism may be responsible for blocks in the South American sector.

In the present paper, the KRM mechanism for the generation and maintenance of blocks is tested by

* On leave from Departamento de Meteorología, Universidad de Buenos Aires and Consejo Nacional de Investigaciones Científicas y Técnicas, Argentina.

Corresponding author address: Dr. Ernesto H. Berbery, Dept. of Meteorology, The University of Utah, 819 Wm. Browning Building, Salt Lake City, Utah 84112.

means of a hemispheric shallow-water model with spherical geometry. This model includes realistic topography for the South American continent. In section 2 a case study of a blocking episode during June 1985 is presented. A description of the model employed is provided in section 3. The results of the numerical experiments are developed in section 4 and a summary and conclusions are contained in section 5.

2. An observational example of a blocking situation

No rigid criteria will be used to define blocking episodes. Rather, focus will be placed upon their most common characteristics that last for several days: a high (or intense ridge) located poleward of the region where they usually are found; a split of the westerlies into two branches and a cutoff low equatorward of the blocking high may also be present.

European Centre for Medium-range Weather Forecasts (ECMWF) analyses will be used to characterize the circulation during the first part of June 1985, when a well-defined block was present in the South American region. Rutllant and Fuenzalida (1987) described from a synoptic point of view this case, in connection with a local contamination episode. Their analysis shows that a ridge advanced from the west and only after it passed the Andes did it intensify. The block occupied the vertical extent of the troposphere with an equivalent barotropic structure and acquired a slight retrogressing movement during the last days of its lifetime.

The following analysis was performed using the 1200 UTC ECMWF data at 300 hPa. Figure 1a shows the 300 hPa geopotential height field averaged over the period 2–9 June 1985. A well-defined ridge is evident near 75°W with troughs located upstream and downstream of the ridge position. Anomalies of the averaged 300 hPa heights relative to the zonal mean are shown in Fig. 1b. Positive anomalies are found in the southern part of South America, eastern Pacific and southwestern Atlantic with the largest anomalies over the Antarctic Peninsula. Strong negative departures are evident near 30°S, 45°W and 40°S, 110°W.

Figure 2 shows a Hovmoeller diagram at 60°S during the first 12 days of June 1985 for the 300 hPa height field. The block remained stationary in longitude near 60°W, having its greatest intensity from 2 through 9 June, with a maximum amplitude on 5 June.

The zonal wind component is averaged for the same period, 2–9 June 1985 (Fig. 3a). The most striking features are the minimum in the westerly flow which becomes slightly easterly wind over a 20° latitude band near Chile and the poleward displacement of the mean jet position. The mean meridional component is computed for the period 2–6 June 1985 (Fig. 3b) to emphasize the early stages of the block. Even though the maximum southerly flow is not located over the mountains, equatorward components of the wind are found over them, with values of approximately 15 m s^{-1} over the region 25°–35°S, 70°–65°W, and increasing to the south to more than 30 m s^{-1}.

The 300 hPa height field averaged over the period 2–9 June 1985 is decomposed into its zonal Fourier components (Fig. 4). All waves 1–4 have positive contributions in the South American region, but wave 2

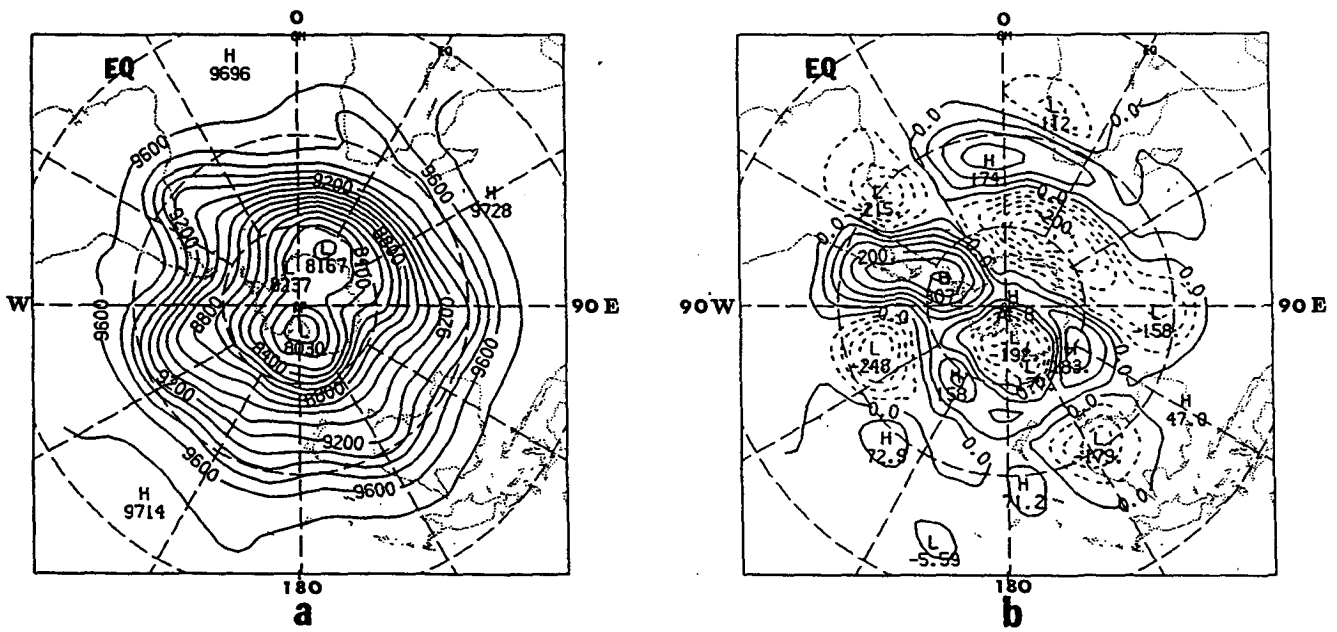

FIG. 1. (a) 300 hPa geopotential height field averaged for the period 2–9 June 1985 (contour interval is 100 m), and (b) its anomalies relative to the zonal mean (contour interval is 50 m). Latitude and longitude lines are every 30°; the outer circle is the equator.

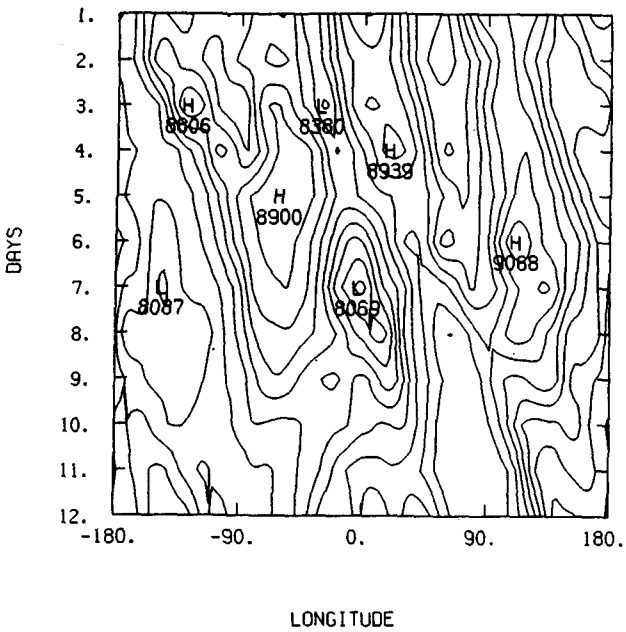

FIG. 2. Hovmoeller diagram at 60°S for the 300 hPa geopotential heights for the period 2–9 June 1985. Contour interval is 100 m.

has the largest amplitude. During this period wave 3 is noticeably weak and does not contribute significantly to the total field.

3. Model description

The model used in this study is based upon the shallow-water equations in spherical coordinates, which can be written in the form (e.g., see Arakawa and Lamb 1981):

$$\frac{\partial}{\partial t}(u/m) - q(h-s)v/m + \frac{\partial}{\partial \lambda}(V^2/2 + \Phi) = 0 \quad (1)$$

$$\frac{\partial}{\partial t}(v/n) + q(h-s)u/n + \frac{\partial}{\partial \phi}(V^2/2 + \Phi) = 0 \quad (2)$$

$$\frac{\partial}{\partial t}(h/mn) + \frac{\partial}{\partial \lambda}[(h-s)u/n] + \frac{\partial}{\partial \phi}[(h-s)v/m] = 0. \quad (3)$$

The first two equations are the momentum equations while the last one is the continuity equation integrated in the vertical. The following symbols are used:

ϕ, λ	latitude, longitude
u, v	wind components
V	wind vector
q	potential vorticity
s	terrain height
h	free surface height
Φ	gh (g: gravity)
m	$[=1/(a\cdot\cos\phi)]$
n	$[=1/a]$
a	the Earth's radius.

The system (1)–(3) is solved by means of the Arakawa and Lamb (1981) scheme for the 300 hPa level. The scheme conserves the total energy and potential enstrophy of the system and does not allow spurious energy cascades to the shorter waves. It also allows the presence of steep mountains, such as the Andes Moun-

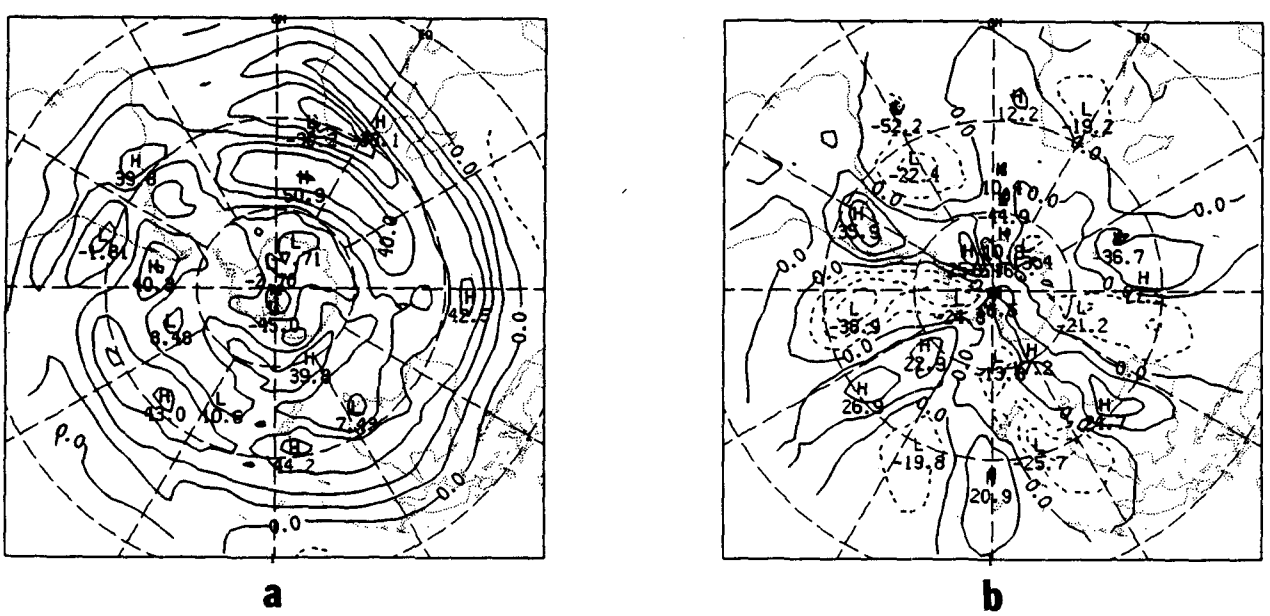

FIG. 3. (a) Zonal wind component averaged for the period 2–9 June 1985 and (b) meridional wind component averaged for the period 2–6 June 1985. Contour interval is 10 m s^{-1}, latitude and longitude lines as in Fig. 1.

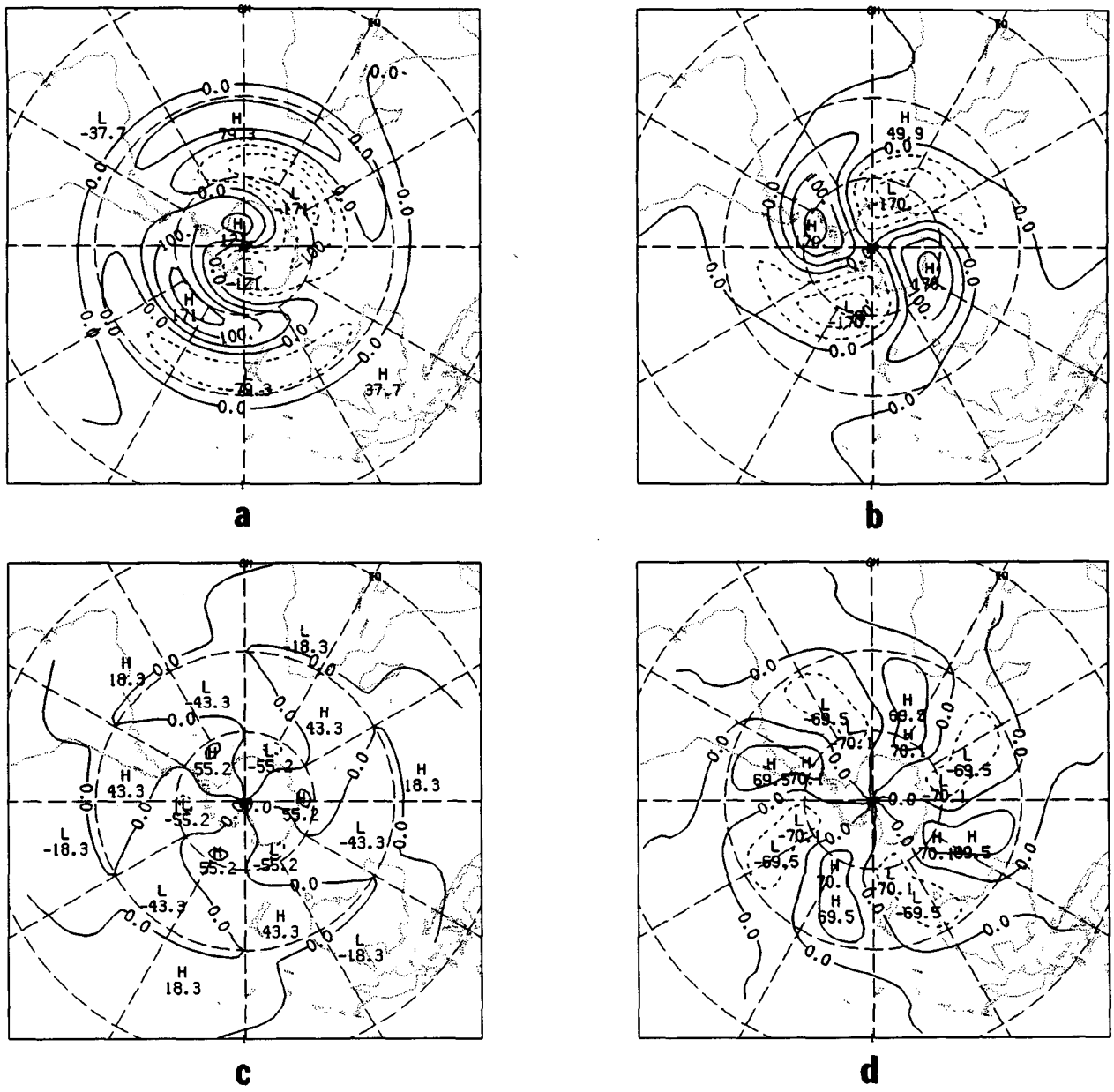

FIG. 4. Decomposition of the mean 300 hPa geopotential height field of Fig. 1a into its zonal Fourier components. (a) wave 1, (b) wave 2, (c) wave 3 and (d) wave 4. Contour interval is 50 m, latitude and longitude lines as in Fig. 1.

tains. The domain of integration is the whole Southern Hemisphere minus a 10° band from the equator. A 5° × 9° latitude–longitude grid is used for the domain of integration.

At the north boundary (at 10°S), it is assumed that no meridional wind exists ($v_b = 0$), and that there is geostrophic equilibrium between the zonal wind and the height.

To avoid linear instability near the South Pole, a Fourier filter was employed to the south of 60°S, following Holloway et al. (1973). Envelope orography (the mean orography plus one times the standard deviation) is employed to represent the Andes Mountains. Thus, the highest peaks exceed 4000 m (Fig. 5), a value which is more realistic than that resulting from mean orography alone. However, due to the coarse grid, the mountains in the model have a greater longitudinal extension than the real ones.

4. The experiments

For the following experiments an initial constant zonal wind profile of 15 m s^{-1} is used; the Andes Mountains act as the downstream forcing while a

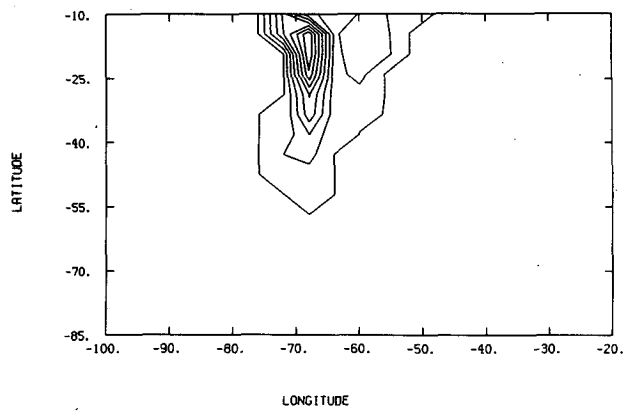

FIG. 5. South American envelope orography used in the numerical experiences. Contour interval is 500 m. The 4000 m contour and the maximum label of 4110 m were omitted.

Gaussian type "mountain," elongated in the meridional direction, is used as an upstream steady forcing in the Pacific Ocean. It has a maximum height of 3000 m at 35°S, 135°W that decays to 1 e^{-1} of that value every 500 and 1000 km approximately in the zonal and meridional directions respectively and extends 2 and 3 grid points in each direction (from the center) respectively. It is indicated by dashed lines in Fig. 6a.

The coarse location of the upstream forcing was estimated computing the wavelength of a stationary Rossby wave at midlatitudes for the initial wind. Considering the necessity for southerly flow over the Andes, the upstream trough should be located at a distance of ¾ wavelength from those mountains, which in this case gives the location at approximately at 110°–115°W. The final position of the upstream forcing was estimated through this value and sensitivity experiences (as described later in this section).

The reason for choosing this upstream forcing was based on the necessity to obtain a source for stationary waves; the model being barotropic, it was hypothesized that there should not be much difference in the way different forcings act on this model as far as they produce a similar effect in the time-averaged solutions (KRM). This is sustained by preliminary experiences in which a low at approximately 115°W was generated every three days through the continuity equation; while the resulting fields were perturbed, the evolution was similar to that to be described here. Furthermore, KRM report of experiences performed with an upstream mountain instead of vorticity pulses, obtaining similar results (these are not shown in their paper). The counterpart in the real atmosphere for the upstream forcing is not a mountain but any other type of forcing (such as those mentioned in section 1) that will produce an equivalent effect.

No other orographic, or any other type of, forcing is considered here. The continental outlines are drawn in the figures for orientation purposes only.

a. Temporal evolution of the simulated blocking

During the first few days of the integration, two troughs can be found downwind of each forcing, with their axes at 115° and 50°W approximately (Fig. 6a). The ridge between them is located just upstream of the Andes, producing southwest wind over those mountains. While the first trough remains almost without any change, the second one deepens and is followed by an equally intense ridge downstream. The evolution of this trough–ridge is such that on day 7 there is a cutoff low to the south of Brazil and a ridge to the east (Fig. 6b). During subsequent days the anticyclone (now fully developed), moves westward and to the south of the low, which remains nearly stationary (Fig. 6c). After day 14 (Fig. 6d) the cutoff low drifts to the east while the blocking high loses its intensity and moves to the north like a ridge over the continent (not shown).

A Hovmoeller diagram of 300 hPa height at 50°S (in the vicinity of the blocking high) is shown in Fig. 7. The two troughs during the initial days of the integration, are evident while the blocking high develops and reaches a large amplitude on day 6 and retrogresses westward during the next 10 days. The observed case (Fig. 2) does not show such retrogression; however, both simulated and observed cases show low height values to the flanks of the high, as is typical in blocking events (Mo et al. 1987). The simulations reproduce about 50% of the pressure gradients between the blocking high and the associated troughs.

b. Mean field

Geopotential heights at 300 hPa are averaged for days 10–15 of the simulation (Fig. 8a). When averaged in time, the cutoff low is zonally elongated with its center at approximately 20°S, 45°W, while the blocking high to the south, is centered at 40°S, 50°–60°W, near the Argentinian coast. In the Pacific Ocean at 110°–120°W, the trough remains near the area of the upstream forcing throughout the integration.

Figure 8b presents the anomalies relative to the zonal mean for days 10–15 of the model integration. The positive anomaly associated with the blocking high is centered near 55°S, 60°W, while the negative anomaly associated with the cutoff low is centered near 20°S, 45°W. A comparison of the model anomaly field (Fig. 8b) with the observed field during 2–9 June 1985 (Fig. 1b) shows that the general pattern is similar. Not only do the locations of positive and negative anomalies correspond to those of the observed blocking high and cutoff low, respectively, there is also good replication of the negative anomaly near approximately 40°S, 115°W.

The zonal wind component averaged for the same period (Fig. 9a) has a region with easterlies to the east of the continent, and a weaker region of westerlies over the Antarctic Peninsula. The intense winds to the north

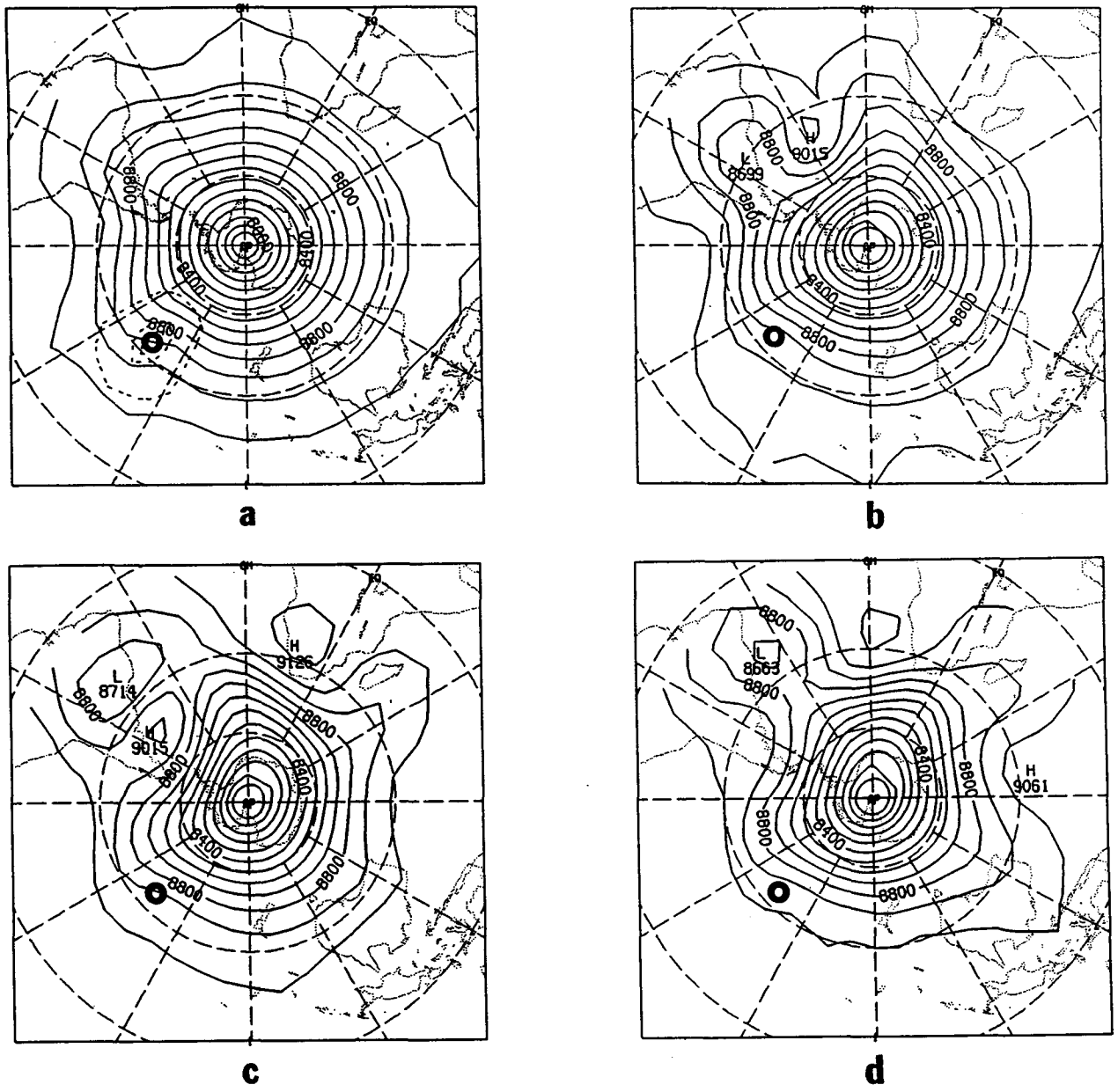

FIG. 6. 300 hPa geopotential height fields for days 2 (a), 7 (b), 12 (c) and 14 (d) of the model integration. Contour interval is 100 m, latitude and longitude lines as in Fig. 1. On Fig. 6a the Gaussian mountain (upstream forcing) is represented by dashed lines, with a contour interval of 1000 m. The small circle represents its center (35°S, 135°W).

of the block seem to be the result of the geostrophic boundary condition at 10°S. The observed case of June 1985 differs in that the easterlies are less intense and located to the west. The mean meridional wind field was computed for days 7 to 10 (Fig. 9b), again to emphasize the early stages of the blocking episode: over the Andes the southerly component of the wind reaches a maximum value of 24.4 m s^{-1}. Comparison with the observed case of June (Fig. 3b) shows a resemblance in the region between 120° and 30°W, with a negative–positive–negative pattern in both observed and simulated cases.

Table 1 summarizes the location of the different positive and negative anomaly centers according to the simulation and for the observed case during June 1985. The same information (where available) is included for the Grandoso and Núñez (1955) case study of June 1952 and the Malaka and Núñez (1980) case of October 1962. (They point out that seven months of that year had the same blocking pattern.) It is evident from

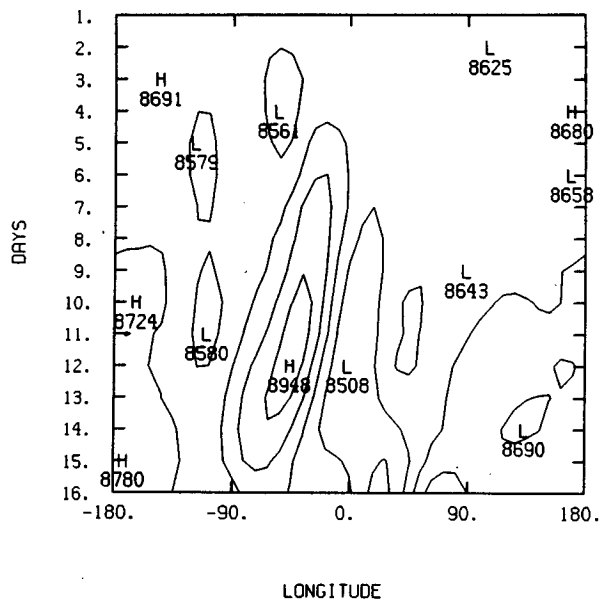

FIG. 7. Hovmoeller diagram at 50°S for the 300 hPa geopotential heights for the first 16 days of the integration. Contour interval is 100 m.

Table 1 that the locations of the blocking high, the cutoff low and the negative anomalies in the Pacific Ocean are similar. The main difference between the simulation presented here and the observed blocking episodes is the equatorward displacement of the simulated blocking pattern, particularly the cutoff low. Also included in Table 1 is the mean meridional wind component between 25° and 35°S, 70° and 65°W that shows (in all the cases in which it was available), the equatorward wind component over the Andes. This is the essential condition under which the KRM mechanism will act.

The studies by Grandoso and Núñez (1955) and Malaka and Núñez (1980) do not provide information over the Pacific Ocean, due to the absence of data in the region; nevertheless, Grandoso and Núñez (1955) show, in their mean field, equatorward directed winds over the Andes.

Note that none of these cases is similar to that studied by Kalnay et al. (1986). They found anomalous large-amplitude short-scale waves in the South American region in January 1979 that were related to active convection on the South Pacific convergence zone. This upstream forcing was further west than that used in our numerical simulations to produce equatorward meridional flow over the Andes. Figure 1a from Kalnay et al. (1986) shows that the mean meridional component of the wind over the Andes for January 1979 was poleward from 10°S past the southern tip of the continent so that the ridge centered north of 40°S at 60°W could not be maintained by the orographic forcing (Kalnay et al. 1986). No blocking was present to the south.

Zonal wavenumbers 1 to 4 for the mean height field are shown in Fig. 10; wave 2 has the highest amplitude in the South American region followed by waves 3 and 4. Waves 5 and 6 (not shown) have small amplitudes, and the overall impression from their temporal evolution is that they do not have any role in the evolution of the block. In the observed case of June 1985, waves 1, 2 and 4 at least double the amplitude of their coun-

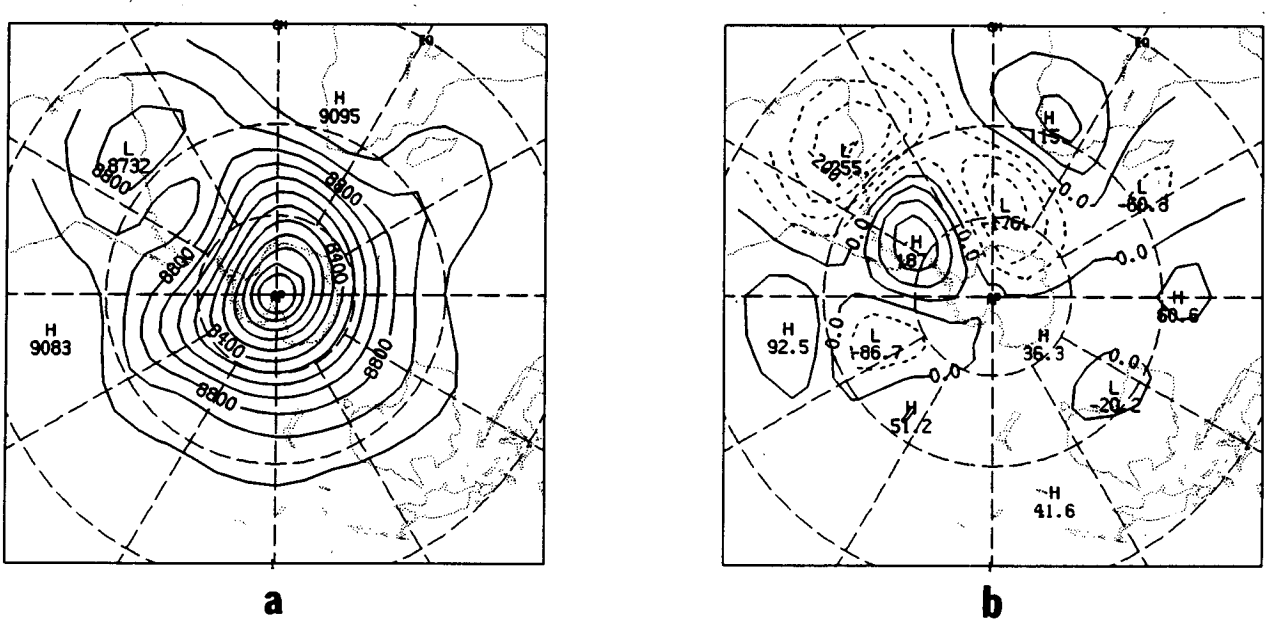

FIG. 8. (a) 300 hPa geopotential height field averaged for days 10–15 of the integration (contour interval is 100 m), and (b) its anomalies relative to the zonal mean (contour interval is 50 m). Latitude and longitude lines as in Fig. 1.

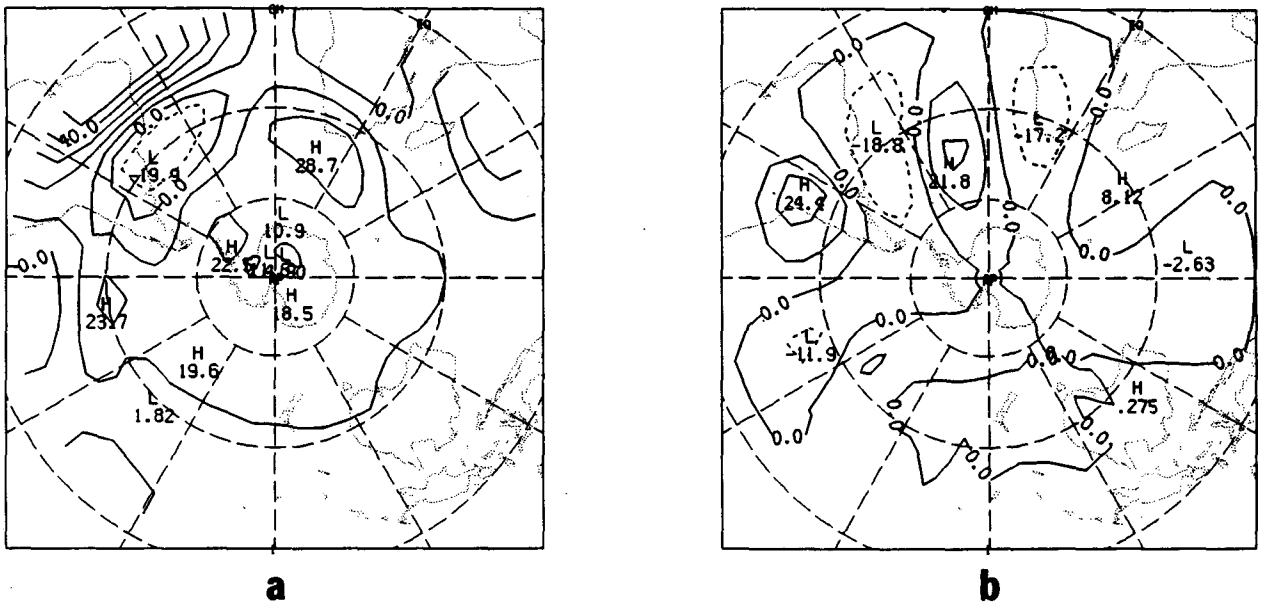

FIG. 9. (a) Zonal wind component averaged for days 10–15 of the integration, and (b) meridional wind component averaged for days 7–10 of the integration. Contour interval is 10 m s^{-1}, latitude and longitude lines as in Fig. 1.

terparts in the simulated block. However, wave 3 has a larger amplitude in the simulation than in the observed case; this does not change the conclusion on the qualitative agreement between both the observed and simulated cases.

The similarity found in the location of the anomalies of the mean field is also present in the comparison of the first four waves of the observed and simulated cases (Figs. 4 and 10). This is particularly so to the south of 30°S. Each wavenumber has almost the same location, even though the amplitudes are different.

TABLE 1. Location of the anomaly centers of the mean field relative to the zonal mean. Abbreviations in the first column mean: SIM, simulation; OBS, observed case in June 1985; GN, Grandoso and Núñez (1955) study of a blocking case occurred in June 1952; MN, Malaka and Núñez (1980) study for October 1962. In the last column, the approximate equatorward wind (meridional component) over the Andes, between 25 and 35°S, 70° and 65°W is shown.

	Atlantic				Pacific		
	Positive anomaly		Negative anomaly		Negative anomaly		
	°W	°S	°W	°S	°W	°S	v (m s^{-1})
SIM	60	55	45	20	110–115	35	14.8
OBS	65	65	50	30	110	35–40	15.7
GN	55–60	60	45	35–40	(1)	(1)	(2)
MN	45	60	50	35	(1)	(1)	(1)

(1) Not given or cannot be estimated from the corresponding papers.

(2) Even though it is not provided in the paper, its figures appear to indicate an equatorward component over the Andes.

c. *Sensitivity studies*

The above results were extended to evaluate the sensitivity of the results to selected model characteristics. First, the sensitivity of the blocking episode to the magnitude of the constant zonal wind is evaluated. If the initial zonal wind is reduced to a zonal velocity of 10 m s^{-1}, then high amplitude waves are produced, but no block. If the initial zonal wind is increased to 20 m s^{-1}, a block is found but only after more than 20 days and in a location that is inconsistent with the observations.

Second, sensitivity to the latitudinal profile of the initial wind field is evaluated. Parabolic wind profiles with a maximum velocity of 15 m s^{-1} at 30° and 55°S (resembling the location of a winter and summer jet stream respectively[1]) are used. However no significant differences with respect to the constant wind profile were found.

Due to the nature of the resonant effects, the longitudinal location of the first forcing is fundamental. A blocking in this model is generated only when the forcing is located near 135°W, so that a trough will be found at approximately 110°–115°W and equatorward flow will prevail over the Andes. If the forcing is shifted by 2 grid points, then no block is observed. The evolution of the blocking episode appeared insensitive to the north–south location of the forcing.

[1] Van Loon (1972), shows that the zonally averaged geostrophic zonal wind for winter at 300 hPa has a maximum of approximately 35 m s^{-1} at 25°–30°S; in summer at the same level, the maximum is of approximately 30 m s^{-1} at 45°–50°S.

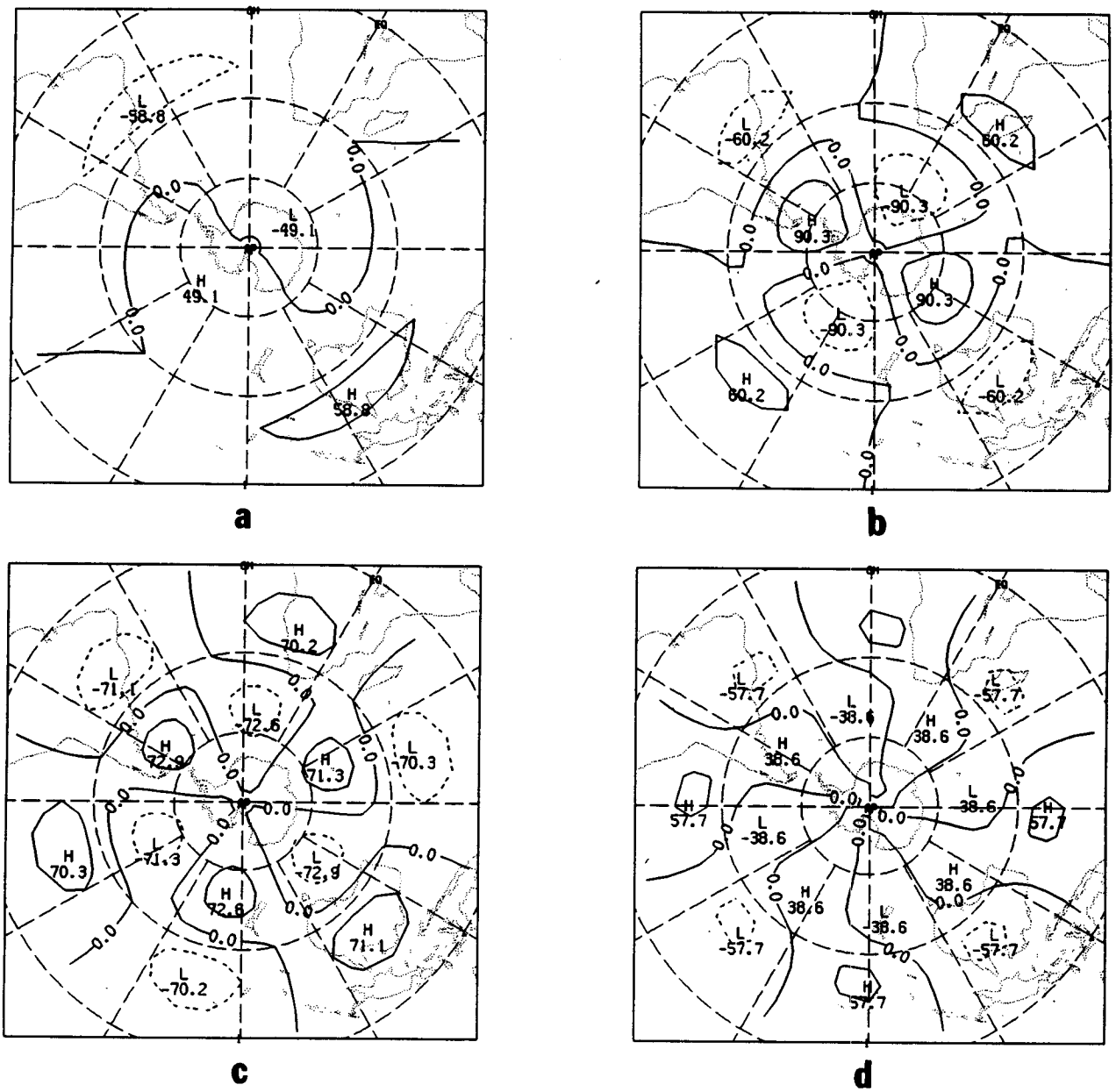

FIG. 10. Decomposition of the mean 300 hPa geopotential height field of Fig. 8a into its zonal Fourier components. (a) wave 1, (b) wave 2, (c) wave 3 and (d) wave 4. Contour interval is 50 m, latitude and longitude lines as in Fig. 1.

5. Summary and conclusions

Several aspects of the simulated block are quite realistic; the overall pattern of the height and wind fields are consistent with the observed block that occurred during June 1985. In addition, the spectral analysis indicates a similar domination of wavenumber 2 during the peak phase of the block. The time evolution of the simulated block differs in some aspects from that observed during June 1985. According to the simulation, the blocking high began and developed over the Atlantic Ocean retrogressing toward the continent. The case during June 1985 does not show such retrogression at the 300 hPa level. However, the simulated block has a similar evolution to a case analyzed by Grandoso and Núñez (1955). According to them the blocking high of their study developed and consolidated over the Atlantic Ocean, retrogressing to the west.

It can be concluded that the KRM mechanism of local resonance is still valid when a model with spherical geometry that is solved in a hemisphere is employed, and when the downstream forcing is the Andes Mountains. This mechanism can explain the blocks initiated in the Atlantic Ocean and also the intensifi-

cation and maintenance of the blocks that develop from a ridge that advances from the west. In this way it provides a simple explanation on how the Andes Mountains can act as a forcing upon the South Atlantic blocking highs. Last, the KRM mechanism can be a useful tool for the forecast of these situations, especially during their later stages.

Acknowledgments. This work was supported by NSF Grant ATM 8613347 and PID 3-916804/85 of the Consejo Nacional de Investigaciones Científicas y Técnicas de la República Argentina (CONICET), and partly represents research completed as a requirement for the first author's Doctorate degree at the University of Buenos Aires. The current work was completed by him with CONICET support at the Department of Meteorology, University of Utah, where he works with Prof. Julia Nogués-Paegle, to whom he is especially indebted. The authors wish also to express their profound appreciation to Dr. John D. Horel, who made several suggestions to enhance and clarify many aspects of this paper.

REFERENCES

Arakawa, A., and V. Lamb, 1981: A potential enstrophy and energy conserving scheme for the shallow water equations. *Mon. Wea. Rev.*, **109**, 18–36.

Baines, P. G., 1983: A survey of blocking mechanisms with application to the Australian region. *Aust. Meteor. Mag.*, **31**, 27–36.

Dole, R. M., 1986: The life cycles of persistent anomalies and blocking over the North Pacific. In Anomalous Atmospheric Flows and Blocking. *Adv. Geophys.*, **29**, 31–69.

——, and N. M. Gordon, 1983: Persistent anomalies of the extratropical Northern Hemisphere wintertime circulation: Geographical distribution and regional persistence characteristics. *Mon. Wea. Rev.*, **111**, 1567–1587.

Grandoso, H., and J. E. Núñez, 1955: Análisis de una situación de bloqueo en la parte austral de América del Sur. *Meteoros*, **5**, 35–54.

Holloway, J., M. Spelman and S. Manabe, 1973: Latitude-longitude grid suitable for numerical time integration of a global atmospheric model. *Mon. Wea. Rev.*, **101**, 69–78.

Kalnay-Rivas, E. and L.-O. Merkine, 1981: A simple mechanism for blocking. *J. Atmos. Sci.*, **38**, 2077–2091.

Kalnay, E., K. C. Mo and J. Paegle, 1986: Large-amplitude, short-scale stationary Rossby waves in the Southern Hemisphere: Observations and mechanistic experiments to determine their origin. *J. Atmos. Sci.*, **43**, 252–275.

Malaka, I., and S. Núñez, 1980: Aspectos sinópticos de la sequía que afectó a la República Argentina en el año 1962. *Geoacta*, **10**, 1–21.

Mo, K. C., J. Pfaendtner and E. Kalnay, 1987: A GCM study on the maintenance of the June 1982 blocking in the Southern Hemisphere. *J. Atmos. Sci.*, **44**, 1123–1142.

Rutllant, J., and H. Fuenzalida, 1987: Bloqueo atmosférico en el cono sur de América conducente a un episodio de contaminación atmosférica en Santiago de Chile. *Proceedings of the 2nd Interamerican Meteorological Congress and 5th Argentinian Meteorological Congress*, Buenos Aires, Centro Argentino de Meteorologos and Amer.

Shukla, J., and K. C. Mo, 1983: Seasonal and geographic variations of blocking. *Mon. Wea. Rev.*, **111**, 388–402.

Taljaard, J. J., 1972: Synoptic meteorology of the Southern Hemisphere, *Meteorology of the Southern Hemisphere. Meteor. Monogr.* No. 35, Amer. Meteor. Soc., 139–211.

Trenberth, K. E., 1986: An assessment of the impact of transient eddies on the zonal flow during a blocking episode using localized Eliassen–Palm flux diagnostics. *J. Atmos. Sci.*, **43**, 2070–2087.

——, and K. C. Mo, 1985: Blocking in the Southern Hemisphere. *Mon. Wea. Rev.*, **113**, 3–21.

van Loon, H., 1956: Blocking action in the Southern Hemisphere. Part 1. *Notos*, **5**, 171–178.

——, 1972: Wind in the Southern Hemisphere, *Meteorology of the Southern Hemisphere. Meteor. Monogr.*, No. 35, Amer. Meteor. Soc., 87–100.